American Journal of
Botany

Quantitative trait locus mapping reveals an independent genetic basis for joint divergence in leaf function, life-history, and floral traits between scarlet monkeyflower (*Mimulus cardinalis*) populations

Thomas C. Nelson[1],* [iD] , Christopher D. Muir[2,3],* [iD] , Angela M. Stathos[1], Daniel D. Vanderpool[1], Kayli Anderson[1], Amy L. Angert[2] [iD] , and Lila Fishman[1,4] [iD]

[1] Division of Biological Sciences, University of Montana, Missoula, Montana 59812, USA

[2] Departments of Botany and Zoology and Biodiversity Research Centre, University of British Columbia, Vancouver, British Columbia V6T 1Z4, Canada

[3] School of Life Sciences, University of Hawai'i, Honolulu, Hawai'i 96822, USA

[4] Author for correspondence (e-mail: lila.fishman@mso.umt.edu)

*Equal contribution

PREMISE: Across taxa, vegetative and floral traits that vary along a fast-slow life-history axis are often correlated with leaf functional traits arrayed along the leaf economics spectrum, suggesting a constrained set of adaptive trait combinations. Such broad-scale convergence may arise from genetic constraints imposed by pleiotropy (or tight linkage) within species, or from natural selection alone. Understanding the genetic basis of trait syndromes and their components is key to distinguishing these alternatives and predicting evolution in novel environments.

METHODS: We used a line-cross approach and quantitative trait locus (QTL) mapping to characterize the genetic basis of twenty leaf functional/physiological, life history, and floral traits in hybrids between annualized and perennial populations of scarlet monkeyflower (*Mimulus cardinalis*).

RESULTS: We mapped both single and multi-trait QTLs for life history, leaf function and reproductive traits, but found no evidence of genetic co-ordination across categories. A major QTL for three leaf functional traits (thickness, photosynthetic rate, and stomatal resistance) suggests that a simple shift in leaf anatomy may be key to adaptation to seasonally dry habitats.

CONCLUSIONS: Our results suggest that the co-ordination of resource-acquisitive leaf physiological traits with a fast life-history and more selfing mating system results from environmental selection rather than functional or genetic constraint. Independent assortment of distinct trait modules, as well as a simple genetic basis to leaf physiological traits associated with drought escape, may facilitate adaptation to changing climates.

KEY WORDS annuality; *Erythranthe*; leaf economics spectrum; leaf physiology; mating system; Phrymaceae; QTL mapping; tradeoff.

Unrelated plant taxa often converge on suites of correlated traits, such as the floral selfing syndrome (Sicard and Lenhard, 2011) or points along the leaf economics spectrum (Wright et al., 2004). Similar spectra sometimes exist within genera and species, with parallel variation in physiological, morphological, and life-history traits across environmental gradients (Mason and Donovan, 2015; Muir et al., 2017; Anderegg et al., 2018; Fajardo and Siefert, 2018; Sartori et al., 2019; Ji et al., 2020). Consistent trait correlations across taxa may arise from fundamental genetic constraints mediated by developmental and physiological tradeoffs. If so, trait syndromes

evolve via alleles with pleiotropic effects on multiple traits (Troth et al., 2018; Martínez-Berdeja et al., 2020), establishing strong genetic correlations that may constrain or accelerate adaptation to novel environmental conditions depending on the direction of multivariate selection. Alternatively, convergent integration of traits across gradients may reflect independent local adaptation by individual traits to shared environmental factors in the absence of any necessary functional connection (reviewed in Donovan et al., 2011; Agrawal, 2020; Guilherme Pereira and Marais, 2020). These different genetic bases for trait associations within species imply

that distinct processes could underlie current patterns of diversity and also make divergent predictions about evolutionary responses to environmental change. Therefore, characterizing the genetic architecture of trait syndromes is crucial to understanding the origins and consequences of adaptive covariation among traits.

Along with life history and phenology, leaf functional traits are key mediators of plant adaptive and plastic responses to climatic and geographic variation. Across taxa, it has been posited that resource tradeoffs constrain plants to fall along a single fast-slow axis of resource gain and expenditure (the leaf economics spectrum or LES); taxa on the slow end of the spectrum invest in long-lived leaves with high leaf mass per area (LMA) but relatively low rates of carbon assimilation (photosynthetic rates) and expenditure (growth), whereas those on the fast end produce leaves with faster rates of both metabolism and turnover (Reich et al., 1997; Wright et al., 2004). The LES has been demonstrated across large taxonomic and geographic scales (Reich et al., 1997; Wright et al., 2004; Díaz et al., 2016), and it has been suggested that correlations among LES traits reflect fundamental physiological or structural constraints (Shipley et al., 2006; Vasseur et al., 2012). Indeed, assays of phenotypic selection and genetic correlations in desert annuals suggest a lack of plants with the (favored) trait combinations that could break LES correlations (Kimball et al., 2013; Angert et al., 2014). However, intra-specific variation in leaf functional traits often does not fully recapitulate the LES (Anderegg et al., 2018; Derroire et al., 2018), particularly in herbaceous taxa (Mason and Donovan, 2015; Muir et al., 2017; Agrawal, 2020; Ji et al., 2020). Thus, it is often not clear what ecological and evolutionary processes (e.g., constraint, natural selection, and/or plasticity) generate large-scale patterns of trait correlation among leaf traits, preventing prediction of evolutionary responses to novel conditions.

Beyond the controversy over the origins of correlations among leaf traits, the extent to which leaf-level physiology constrains organism-level ecological strategies (or vice versa) remains unclear. Based on cross-taxon correlations, the fast-slow LES axis of resource acquisition has been argued to underpin a parallel fast-slow life history axis (Adler et al., 2014; Salguero-Gómez, 2017). Consistent with a fundamental relationship, leaf functional traits exhibit the predicted correlations with life-history and climate (growing season length) across accessions of the model annual plant *Arabidopsis thaliana* (L.) Heynh. [Brassicaceae] (Sartori et al., 2019). Similarly, photosynthetic physiology correlates with mating system across closely-related *Clarkia* species, perhaps because rapid-cycling annuals require greater reproductive assurance in a temporally constrained growing season that also favors a fast life history and resource-acquisitive leaf traits (Mazer et al., 2010). It is tempting to conclude that such cross-population associations, as well as larger scale patterns, arise from genetic correlations caused by pleiotropy (multiple effects of single genes) or tight linkage (Lowry and Willis, 2010). However, despite abundant heritable variation in leaf functional traits within species (Ackerly et al., 2000; Geber and Griffen, 2003; Guilherme Pereira and Marais, 2020), there is little evidence of genetic coordination among them (Muir and Moyle, 2009; Muir et al., 2014; Taylor et al., 2016; Coneva et al., 2017; Coneva and Chitwood, 2018). Evidence of genetic coordination of physiology or leaf structure with fast-slow traits at the whole-plant level has been even more elusive (Ivey et al., 2016). However, the genetics of both leaf functional traits and life history variation remain poorly understood outside a few model systems (reviewed in Guilherme Pereira and Marais, 2020), and further investigation of the joint genetic architecture of leaf-scale and whole-organism traits within species is needed.

Here, we use a line-cross approach and quantitative trait locus (QTL) mapping to examine the genetic architecture of inter-population divergence in leaf function, life-history, and reproductive (mating system) traits in the riparian plant *Mimulus (sect. Erythranthe) cardinalis* Dougl. ex Benth. The hummingbird-pollinated *M. cardinalis* (and its close relative *M. lewisii* Pursh, which is bee-pollinated) are well-established models for understanding the evolution of pollination syndromes (Hiesey et al., 1971; Bradshaw et al., 1995; Bradshaw and Schemske, 2003; Yuan et al., 2016) and elevational adaptation (Hiesey et al., 1971; Angert, 2006), as well as species barriers (Ramsey et al., 2003; Fishman et al., 2013; Stathos and Fishman, 2014). Physiological and demographic variation across the wide *M. cardinalis* latitudinal range is also unusually well-characterized, making it a model for understanding herbaceous plant responses to rapid climate change (Angert et al., 2011; Sheth, 2016; Muir and Angert, 2017; Sheth and Angert, 2018). Across its latitudinal range from Baja California to Oregon, *M. cardinalis* occurs in flowing-water riparian habitats, which vary substantially in the timing and magnitude of water availability. Because *M. cardinalis* cannot survive complete dry-down during its vegetative growing season (Sheth and Angert, 2018), latitudinal variation in water availability should strongly shape population differences in life history, phenology, and mating system, as it does physiological traits such as photosynthetic assimilation rate (Muir and Angert, 2017). We focus here on variation represented by parental plants sampled from two region of California, a Sierran montane site and a southern desert-scrub site; these populations are separated by only ~1/3 of the latitudinal range of *M. cardinalis*, but differ substantially in precipitation/temperature regimes and represent distinct biogeographic clades in population genomic analyses (Nelson et al., 2021b).

In order to quantify the genetic architecture of trait correlations, as well as identify genomic regions contributing to divergence in single or multiple traits, we took a multi-step approach. First, we estimated quantitative genetic parameters (broad-sense heritability and genetic covariances) for 20 traits using an inbred line-cross approach with parental and F_1 replicates and segregating F_2 hybrids (N = 200). By estimating environmental correlations (r_E) from covariance among traits within the three genetically homogenous genotypic classes, we can estimate genetic correlations (r_G) in F_2s. Although epistasis and genotype × interactions may generate substantial line-cross r_G in the absence of linkage or tight pleiotropy, low values of r_G allow us to reject strong functional constraints as the cause of cross-population associations between fast-slow axis traits. Second, we generated the first intra-specific linkage map for *Mimulus* section *Erythranthe* using high-density gene-capture markers suitable for scaffolding the draft genome sequence of the species into chromosomes (n = 2152 loci, N = 93 genotyped F_2s). Third, we mapped primary QTLs underlying the 20 traits to determine their individual genetic architecture, then screened for secondary QTLs at a lower statistical threshold and asked whether QTLs for multiple traits co-localize. Although 93 F_2 individuals do not provide high resolution for characterizing the full number and effect size of QTLs for polygenic traits (Beavis, 1994), this approach provides power to identify major or leading QTLs for individual traits and to rule in or out the possibility that any given trait pair is under the control of major pleiotropic or tightly linked loci, complementing genome-wide inferences from the larger quantitative genetic dataset. Together, this work provides insight into genetic architecture of individual adaptive traits as well as the origins of functional trait syndromes and

provides a platform for predicting how *M. cardinalis* populations can evolutionarily respond to rapidly changing climatic conditions.

MATERIALS AND METHODS

System and plant materials

Mimulus cardinalis (Phrymaceae), also known as *Erythranthe cardinalis* (Dougl. ex Benth.) Spach (Barker et al., 2012), but see (Lowry et al., 2019), is a hummingbird-pollinated herbaceous plant of low elevation riparian habitats in western North America. Across its latitudinal and elevational range from Baja California to Oregon, *M. cardinalis* varies extensively in life history and functional traits (Muir and Angert, 2017; Sheth and Angert, 2018). In particular, plants from seasonally dry southern populations grow faster and have higher photosynthetic rates than those from wetter northern populations in field common gardens, consistent with an evolutionary shift toward an annualized life history in southern habitats where precipitation is both less available on average and less predictable across years (Muir and Angert, 2017). Demographic studies in the wild confirm adaptive divergence in life history, with southern populations experiencing higher annual mortality but greater reproduction at small size than central (Sierran) populations (Sheth and Angert, 2018). We focus here on representative lines from Sierran (CE10: a well-characterized inbred line derived from the Carlon population along the South Fork Tuolumne River in the Sierra Nevada Range near Yosemite National Park; Bradshaw and Schemske, 2003) and Southern (WFM: West Fork Mohave River; Fishman et al., 2013; Muir and Angert, 2017) regions.

Growth conditions, phenotyping, and quantitative genetic analyses

We crossed CE10 (as dam) with WFM 1.1 (a single plant grown from wild-collected seed) to generate F_1 hybrids, and then hand-self-pollinated a single F_1 to generate a segregating F_2 population. In Fall 2013, F_2 hybrids (N = 200 total) were grown in a greenhouse common garden at the University of Montana along with replicates of the parental lines (WFM 1 generation inbred) and F_1 hybrids (N = 25 each). Seeds from each genotypic class were sown on wet sand in separate, parafilm-sealed Petri dishes, with seedlings transplanted into 96-cell growth trays after 10 days (treated as germination time, Day 0) and the entire plugs transferred into 4-inch pots filled with Sunshine Mix #1 (Sungro Horticulture, Agawam, Massachusetts, USA) at one month after initial sowing. Plants were maintained in randomized arrays with daily bottom-watering, bi-weekly ½ strength fertilization with Peters Professional 20-20-20 fertilizer (ICL Specialty Fertilizers, Summerville, South Carolina, USA), moderate temperatures (80/65°F day/night), and supplemental lighting to maintain a long-day photoperiod (16h day/8h night).

To estimate plant size and growth rate, we recorded height (mm) at one time point (Day 45 post-germination) and basal stem diameter (BSD) at two time points 3 weeks apart (Day 33 and Day 55 post-germination), from which we calculated adult relative growth rate (RGR = $[\ln(BSD2) - \ln(BSD1)] / (t_2 - t_1)$). BSD2 and BSD1 are the basal stem diameters at times t_2 and t_1, respectively. At the time of height measurement, we also scored whole plants semi-quantitatively (ordinal 0-3 scale, with the extremes defined by the parental replicates) for stem anthocyanin production (RedStem). Vegetative anthocyanins may mitigate abiotic stresses (Steyn et al., 2002) and anthocyanin polymorphisms are also associated with life history variation in other monkeyflowers (Lowry et al., 2012). For the first flower to open in each plant (beginning Day 52), we recorded days from germination to flower and measured the length of the gynoecium (distance from pedicel to stigma lobes) and androecium (distance from the pedicel to top of tallest anther). These measures of flower length were used to calculate stigma-anther distance, which generally influences autogamous self-pollination ability (Barrett, 2002).

Midday photosynthetic rate (A_{area}, µmol CO_2 m^{-2} s^{-1}), stomatal resistance to water vapor ($r_{sw} = 1/g_{sw}$), and instantaneous water-use efficiency (iWUE = A/g_{sw}) were measured on a single leaf (ranging from the 3rd-5th node) over a series of five days (Days 44-49) using an open-path infrared gas exchange analyzer (LI-6400XT portable photosynthesis system, LI-COR Inc., Lincoln, Nebraska, USA). We analyzed stomatal resistance (r_{sw}, m^2 s mol^{-1}) rather than conductance because the former was normally distributed, whereas the latter was right-skewed. Conditions in the leaf chamber were as follows: leaf temperature = 25°C; CO_2 = 400 ppm; relative humidity = 0.5-0.75; PAR = 400 µmol quanta m^{-2} s^{-1} (close to ambient for greenhouse in midday); and moderate flow rate (300 umol/s). Leaf functional traits (Day 54), including area (cm^2), fresh (leaf fresh mass, g) and oven-dried (leaf dry mass, g) weights, were recorded for the paired leaf from the same node as that measured for gas exchange. We calculated LMA (leaf dry mass /area), leaf dry matter content (LDMC; leaf dry mass/leaf fresh mass) and a proxy for leaf thickness (LMA/LDMC or fresh mass/area, µm) (Vile et al., 2005). Approximately one month after the last plant had initiated flowering (Day 107 from germination), we removed plants from their pots and counted all rhizomes (belowground-initiated vegetative shoots) > 3 cm long. The total aboveground biomass (not including rhizomes) was oven-dried and weighed (biomass, g).

We compared parental and hybrid means and variances, calculated broadsense heritability (H^2), and estimated the environmental (r_E) and genetic (r_G) correlations among traits with $H^2 > 0.20$ following Fishman et al. (2002). Briefly, r_E is calculated from the standardized phenotypic covariances among traits in the genetically invariant parental and F_1 classes, and then r_G is calculated from the F_2 covariances assuming equivalent r_E in the segregating F_2 genotypes. For rhizome number, which was very right-skewed in the F_2s (many zero values, diverse higher values), we log-transformed the raw counts (+ 1) for these calculations (and later QTL mapping). For the leaf functional traits, individual values may be influenced by ambient conditions and ontogeny. To test for such effects, we conducted analyses of variance (ANOVA) on the full dataset for each trait, including sampling date of physiological measures (date) and leaf pair as factors along with genotypic class. Date was a significant factor (all $P < 0.005$) for all of the leaf traits, but leaf pair had no significant effect. Therefore, for the calculations of H^2, r_E and r_G for leaf traits, we use the residuals from an ANOVA with date as a fixed factor. However, because genotypic classes were evenly distributed across sampling dates, removing this additional (co-) variance had no qualitative or statistical effect on differences among the parental and F_1 trait means. Therefore, we present un-standardized means and standard errors for each genotypic class in Table 1. We also ran the QTL analyses (below) for the leaf functional traits with both date-standardized and raw values; however, because these analyses were not qualitatively different in the number or location of QTLs,

TABLE 1. Means (± 1 SE) for life-history, leaf function, and floral traits in *M. cardinalis* parental lines and hybrids, plus broad-sense heritability (H^2). Significant differences among the parental and F_1 classes are indicated by superscripts. Statistical analyses and H^2 calculations were performed on [log (rhizomes + 1)] for rhizomes and date-standardized values for the leaf function traits. For some traits, the number of measures is slightly lower than the total number of plants (minimum N = 22 for parents and F_1s and 197 for F_2s). For traits where the literature predicts a fast-slow axis of trait co-variation, we have bolded the parental trait value with the significantly more resource-acquisitive leaf function and/or fast life history.

Trait	CE10 (sierran) (N = 22)	F_1 hybrid (N = 25)	WFM (Southern) (N = 25)	F_2 hybrids (N = 200)	H^2
Life history (LH)					
Basal stem diameter 1 (BSD, mm)	1.88 ± 0.08[a]	2.84 ± 0.05[c]	2.40 ± 0.07[b]	2.62 ± 0.03	0.54
Basal stem diameter 2 (BSD2, mm)	4.14 ± 0.11[a]	5.16 ± 0.13[b]	5.71 ± 0.09[c]	5.06 ± 0.05	0.13
Relative growth rate (RGR)	0.355 ± 0.026[b]	0.258 ± 0.014[a]	0.380 ± 0.010[b]	0.290 ± 0.006	0.20
Height (cm)	41.6 ± 2.4[a]	80.4 ± 2.8[b]	70.2 ± 4.0[b]	74.4 ± 1.7	0.61
Days to flower	**59.1 ± 0.6**[b]	54.5 ± 0.5[a]	63.1 ± 0.8[c]	56.9 ± 0.3	0.41
Rhizomes	4.76 ± 0.51[c]	3.08 ± 0.37[b]	0.36 ± 0.13[a]	1.96 ± 0.14	0.48
Aboveground biomass (g)	14.48 ± 0.25[a]	16.25 ± 0.29[b]	17.49 ± 0.4[c]	16.61 ± 0.13	0.29
Stem anthocyanin (RedStem)	0 ± 0[a]	0.8 ± 0.13[b]	2.72 ± 0.09[c]	1.25 ± 0.07	0.76
Leaf function (LFunct)					
Assimilation (A_{area}; μmol co_2 m^{-2} s^{-1})	10.88 ± 0.3[a]	11.02 ± 0.28[a]	12.31 ± 0.23[b]	11.47 ± 0.11	0.25
Stomatal resistance (r_{sw}; m^2 s mol^{-1})	2.80 ± 0.18[b]	2.07 ± 0.09[a]	2.16 ± 0.11[a]	2.52 ± 0.05	0.43
iWUE (mmol CO_2 mol^{-1} H_2O)	29.50 ± 1.44[b]	22.52 ± 0.90[a]	26.34 ± 1.19[a,b]	28.27 ± 0.51	0.42
Leaf wet mass (g)	0.58 ± 0.025[a]	0.64 ± 0.02[a]	0.79 ± 0.024[b]	0.65 ± 0.013	0.60
Leaf dry mass (g)	0.077 ± 0.004[a]	0.092 ± 0.003[b]	0.095 ± 0.003[b]	0.09 ± 0.002	0.58
Leaf area (cm^2)	27.36 ± 1.00	26.99 ± 0.77	28.86 ± 0.89	27.39 ± 0.49	0.58
Leaf thickness (μm)	**211.1 ± 2.7**[a]	237.0 ± 2.6[b]	274.4 ± 4.1[c]	237.2 ± 1.25	0.20
LMA (g m^{-2})	**28.53 ± 1.11**[a]	34.52 ± 0.93[b]	33.07 ± 0.88[b]	32.95 ± 0.33	0.07
LDMC (%)	13.5 ± 0.5[b]	14.6 ± 0.4[b]	**12.1 ± 0.3**[a]	13.9 ± 0.2	0.10
Flora/mating system (Rep)					
Gynoecium length(mm)	49.16 ± 0.30[c]	47.75 ± 0.32[b]	45.87 ± 0.35[a]	46.21 ± 0.13	0.29
Androecium length (mm)	45.52 ± 0.37[b]	46.58 ± 0.37[b]	43.87 ± 0.26[a]	44.98 ± 0.17	0.47
Stigma-anther separation (mm)	3.64 ± 0.17[c]	1.17 ± 0.22[a]	2.00 ± 0.30[b]	1.23 ± 0.10	0.33

we present the latter analyses here. All phenotypic analyses were performed in JMP 14 (SAS Institute, 2018).

Because values of r_G estimated from line cross data requires the assumption of no genotype × environment or epistatic interactions in the F_2s hybrids and can reflect weak linkage that would not matter in freely recombining populations, we view them as complementary to the QTL analyses. In particular, when the detected QTLs do not account for the parental differences, low or opposed values of r_G may be useful in ruling out predictable pleiotropy (i.e., functional constraints) at many small-effect loci as the cause of cross-population associations among traits.

Genotyping and genetic mapping

Plants were genotyped using a custom probe set designed from the *M. lewisii* LF10 version 1.1 genome assembly (Yuan et al., 2013b; website: www.mimubase.org). The probes targeted exons and adjacent sequence of genes 1:1 orthologous to genes in *M. guttatus* Fisch. ex DC. (2N = 28), which is segmentally syntenic with *M. lewisii* and *M. cardinalis* (2N = 16) despite the difference in chromosome number (2N = 28 vs. 2N = 16; Fishman et al., 2014). To select genes for enrichment, we extracted all coding sequence from the *M. guttatus* version 2.0 annotation (website www.Phytozome.jgi.doe.gov) and used BLAST to find unique hits in the *M. lewisii* version1.1 genome (e-value ≤ 10^{-10} and e-value[best hit] – e-value[second-best] ≥ 10^{-10}). Unique hits were queried against the *M. cardinalis* CE10 version 1.9 assembly (www.mimubase.org); only sequences present in both *M. lewisii* and *M. cardinalis* assemblies were kept. Lastly, we performed reciprocal best-hit BLAST between the *M. lewisii* and *M.*

cardinalis candidate gene sets to filter out close paralogs. The final probe set consisted of 9126 target regions, which all include exon sequence but may also capture neighboring (and potentially more variable) intronic and untranslated regions.

Sequencing libraries were prepared following (Meyer and Kircher, 2010) and using the SeqCap EZ library preparation kit (Roche Nimblegen, Madison, Wisconsin, USA). Briefly, genomic DNA was sheared to ~300 bp using a Covaris E220 UltraSonicator (Covaris Inc. Woburn, Massachusetts, USA), Illumina adaptors (NEBNext, New England BioLabs, Ipswich Massachussetts, USA) were added via blunt-end ligation, and each library was dual-indexed before multiplexing all libraries into a single reaction for target enrichment. Target enrichment was performed following probe manufacturer's protocols. To avoid enrichment of repetitive DNA, we used the universal Developer Reagent C_0T-1 DNA (Roche Nimblegen, Madison, Wisconsin, USA) during probe hybridization. Libraries were sequenced on a single lane of Illumina HiSeq 2500 (PE 125). Raw Illumina reads were quality filtered and trimmed for sequencing adaptors using Trimmomatic (Bolger et al., 2014) and aligned to the version 1.9 draft *M. cardinalis* genome (website http://mimubase.org) using bwa-mem version 0.7.15 (Li and Durbin, 2009). Alignments were filtered for minimum quality scores of 29 using samtools version 1.3 (Li et al., 2009). We then removed potential PCR duplicates and realigned around indels using Picard Tools (website http://broadinstitute.github.io/picard) and called single nucleotide variants with GATK (version 3.3-0-g37228af) (McKenna et al., 2010) following GATK best practices.

We constructed a linkage map of exon-capture markers genotyped in a subset of the CE10 × WFM F_2s (N = 93). The

high-density linkage map was generated in Lep-MAP3 (Rastas, 2017), with imputation of missing genotypes. We removed markers with > 10% missing genotypes and markers with evidence of strong segregation distortion by χ^2 test ($p \leq 0.001$). We assigned markers to linkage groups with a LOD threshold of 13, resulting in eight linkage groups which were ordered by maximum likelihood using the Lep_MAP3 module OrderMarkers2. Lastly, we conservatively removed errors in map order by assigning the same genetic position to markers within 1000 bp of each other (i.e., from the same targeted capture region). Linkage groups were numbered and oriented in accordance with previous *Erythranthe* section maps (Fishman et al., 2013). For QTL mapping, the full dataset was pruned to 720 recombination-informative sites. To identify QTLs, we conducted single interval scans in rQTL2 (scan1, HK method) (Broman et al., 2003), setting trait-specific LOD thresholds for QTL significance with 1000 permutations of the genotype-phenotype matrix. Because we have only moderate power to detect individual QTLs due to low F_2 sample size, we used a 2-stage approach to identify multi-trait QTLs. First, we identified primary QTLs for each trait significant at experiment-wide $\alpha = 0.05$ (LOD = 3.54–3.77, depending on trait). We then also identified secondary significant QTLs at a less stringent $\alpha = 0.15$ (overlapping LOD = 3.01–3.12). QTLs were considered co-localized if their 1.5 LOD-drop intervals overlapped. Because QTL coincidence is necessary (but not sufficient) for the inference of pleiotropy, this generous second threshold reduces the chance that we will reject a shared genetic basis for traits due to low power to detect QTLs. For trait combinations whose major QTLs do not co-localize, and which also do not show strong (and parallel) genetic correlations in F_2s, we can infer that cross-population trait associations do not reflect pleiotropy or tight linkage.

RESULTS

Parental differences

In our greenhouse common garden, the parental lines exhibited striking differences in whole plant life-history/growth traits, leaf functional traits, and floral traits associated with mating system (Table 1, Fig. 1). The Sierran CE10 line was characteristically perennial in its growth form, producing abundant rhizomes, whereas Southern WFM1 exhibited annual or "faster" life-history traits. Relative to CE10, WFM was taller and larger in basal stem diameter (BSD) at both time points (Table 1). However, because WFM was larger at the first measurement of BSD (suggesting more early growth or earlier germination), relative growth rates over the 3-week adult measurement interval did not differ. Most WFM individuals had made no rhizomes by the end of the entire 15-week growth period, instead achieving >20% greater aboveground biomass. The only life-history trait that broke the typical annual-perennial pattern of differentiation was flowering time, with WFM flowering 4 days later than CE10 plants.

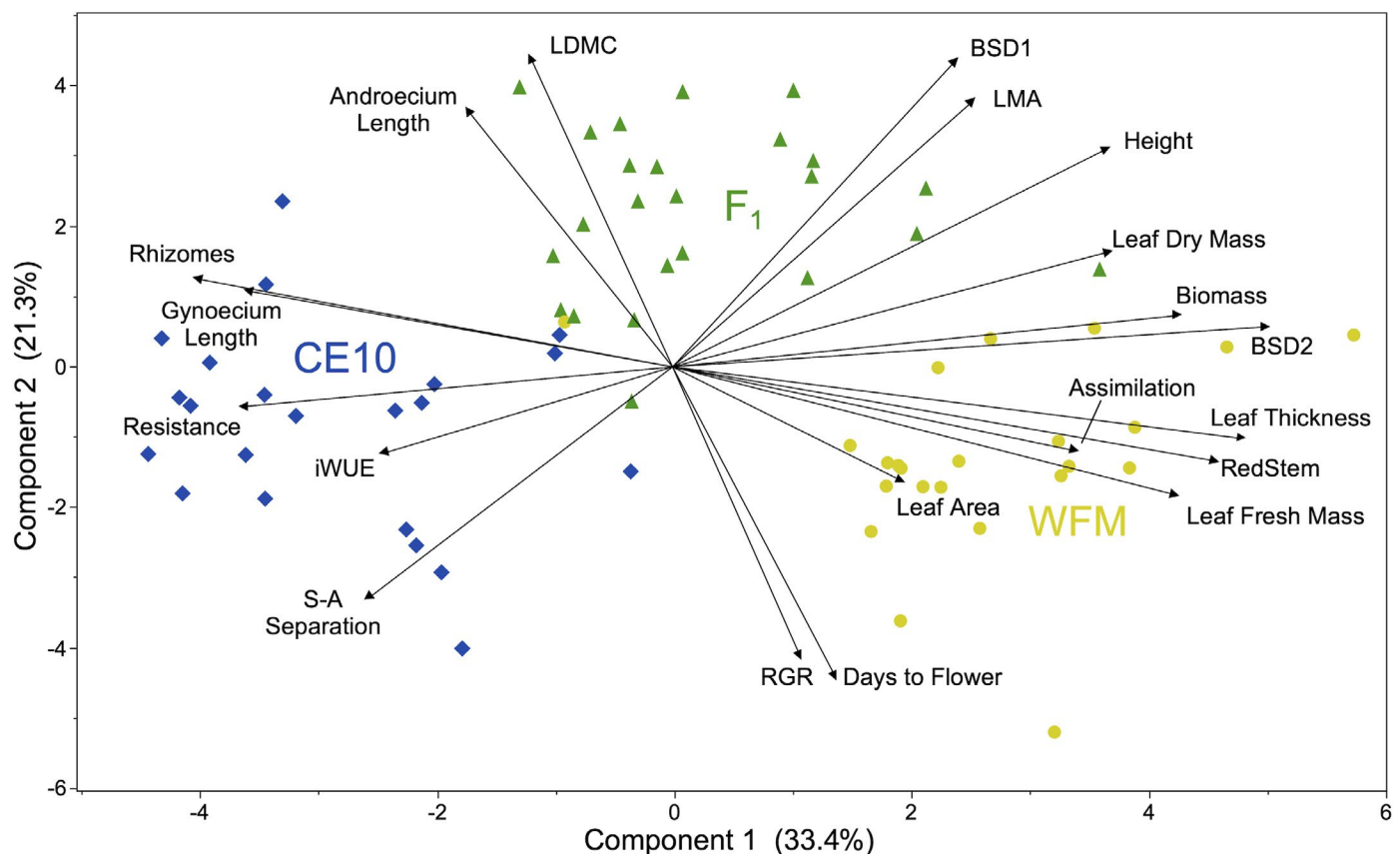**FIGURE 1.** Plot of the first two principal components (PCs) of phenotypic covariation in parental and F_1 hybrid classes of *Mimulus cardinalis* (points show individuals, with shapes and colors indicating their genotypic class). PC1 captures the major axis of parental divergence in life history, floral and leaf functional traits, whereas PC2 is loaded by traits exhibiting transgressive variation in F_1 hybrids.

Parental lines also differed for physiological and leaf traits consistent with life history adaptation to ephemerally wet (WFM) vs. mesic (CE10) habitats (Table 1). WFM exhibited a strong anthocyanin flush on its stems (mean score 2.72 out of 3), whereas CE10 plants did not flush (all 0s). WFM leaves had higher photosynthetic assimilation rate (A_{area}; $P < 0.001$, Table 1) and lower stomatal resistance to water loss (r_{sw}; $P = 0.001$), consistent with a live-fast, die-young strategy. This translated into lower instantaneous water use efficiency (iWUE) in WFM under well-watered greenhouse conditions. Although the parental lines did not differ significantly in leaf area ($P = 0.24$), WFM leaves had 36% greater wet mass ($P < 0.0001$), 25% greater dry mass ($P < 0.005$), and 15% greater leaf mass per area (LMA; $p < 0.005$) than CE10 leaves. The greater fresh leaf bulk of WFM vs. CE10 reflects increased water content and/or laminar thickness ($P < 0.005$) rather than higher tissue density, as WFM actually had 10% lower LDMC ($P = 0.01$).

WFM had overall smaller flowers than CE10 (>3.2 mm shorter gynoecium, ~1.6 mm shorter androecium) and significantly lower stigma-anther separation (Table 1), consistent shift towards increased autogamous selfing capacity in plants from the drier and more variable southern habitat.

Heritabilities and genetic covariances in hybrids

Most traits differentiated between the parents exhibited overall additivity (F_1 and F_2 hybrids, on average, intermediate between parents) or dominance (F_1 hybrids equivalent to one parent, distinct from the other) (Table 1). However, F_1s exhibited transgressive variation (means significantly higher or lower than either parent) for days to flower, basal stem diameter at time 1 (BSD1) and relative growth rate (RGR). F_1s grew faster at early stages (prior to the measurement of BSD1) and flowered earlier than either parent, then grew more slowly in the BSD1-BSD2 interval. In addition, photosynthetic rate and stomatal resistance exhibited opposite patterns of dominance, with F_1s matching the low parent of each trait and thus having transgressively low water use efficiency (iWUE) (Table 1). Stigma-anther separation was similarly transgressive, with F_1s having unexpectedly low stigma-anther separation (Table 1).

Broadsense heritabilities (H^2) were high for the life history traits of flowering date, early growth (BSD1), height, and (log) rhizome number (all >0.40), intermediate for RGR (0.20) and final biomass (0.29), and low for BSD2 (0.13) (Table 1). The essentially Mendelian trait of stem anthocyanin had the highest H^2 (0.76), but leaf size traits (dry mass, wet mass, and area) were also highly heritable ($H^2 > 0.58$). The high heritability for leaf area (despite no parental mean difference) reflects high segregating variance in the F_2 hybrids for all leaf size traits (including transgressive values well outside the range of the other classes). Leaf physiological traits (photosynthetic rate, stomatal resistance, and iWUE) and leaf thickness, as well as floral traits, all had moderate to high values of H^2 (0.20–0.50; Table 1). In contrast, the composite LES traits of LMA and LDMC had low H^2 (<0.10).

As expected, functionally linked traits (e.g., photosynthetic rate and stomatal resistance) tended to show high genetic (r_G) and environmental (r_E) correlations (Fig. 2). However, the decomposition of r_G and r_E also revealed high r_G among traits with no environmental correlation in the parental and F_1 plants (e.g., photosynthetic rate and flowering date). The latter is consistent with genetic correlation due to linkage or pleiotropy, in the absence of any environmental covariance. However, because estimation of r_G from F_2 line cross

data requires the assumption of no shift in the covariance matrix or gene × environment or gene × gene (epistatic) interactions, high values for r_G do not necessarily imply strong genetic constraints. Even weak linkage among underlying loci in F_2s can generate high r_G if Cov_E (plastic covariation within the genetically invariant classes) is near zero or opposite in direction to the genetic associations. For example, r_G is as highly negative for the (functionally unrelated) trait pair of stomatal resistance and stigma-anther separation as it is for resistance and its functional partner photosynthetic rate, likely due to linkage between separate leaf physiology and floral QTLs (see below). Despite this limitation, the absence of strong genetic correlations can reject uniform pleiotropy that constrains plants to adhere to a fast-slow axis of both life history and leaf function. Indeed, life history and growth traits that are positively associated with "fast" leaf traits across the parental lines often had r_G opposite to that expected from pleiotropic constraint (e.g., WFM had relatively high BSD1 and photosynthetic assimilation, but those traits are—if anything—negatively genetically correlated; Fig. 2). Therefore, although it remains possible that individual loci exhibit pleiotropy or linkage (but not uniformly, so as to not produce strong genome-wide r_G), QTL mapping is necessary to tease apart any correlated effects of individual genomic regions.

Linkage and QTL mapping

The sequence-based genotyping yielded 8100 informative single nucleotide polymorphisms (SNPs) across 2152 gene-capture targets. Genetic mapping resolved the expected 8 linkage groups, with 720 unique (at least 1 recombinant in 186 meioses) marker positions spanning a total of 537 cM (Fig. 3). Overall, the mapped markers exhibited mild but significant (at $\alpha = 0.005$ level, to control for multiple non-independent tests) transmission ratio distortion in six regions across five of the chromosomes. All of the distorted regions were characterized by excess heterozygosity (>60%), perhaps due to weak selection against homozygotes (due to inbreeding depression or possibly epistatic incompatibility; Fishman and McIntosh, 2019), and two also had a significant deficit of WFM alleles (<42%). In these most extreme cases, on Chromosomes 2 and 4, the frequency of the rarer WFM homozygote was ~10% (9/93 F_2s) rather than the expected 25%.

We detected 16 primary QTLs for 10 traits (genome-wide $\alpha = 0.05$), and six more overlapping QTLs (at secondary $\alpha = 0.15$ threshold) for a total of 13 traits (Fig. 3, Table 2). For life-history traits, we detected QTLs in four regions, with all but one affecting multiple traits. On Chromosome 1, a multi-trait life-history QTL cluster (LH1) was significantly associated with BSD1, height, and days to flower, and (less strongly) relative growth rate (but not BSD2). This QTL cluster explains 15% to 20% of the variance for traits with moderate (0.2–0.6) heritability, and Sierran CE10 alleles appear recessive. The allelic effects at LH1 are in the expected direction (e.g., CE10 genotypes growing slowly early and reaching shorter heights) for all traits except flowering time (which is instead consistent with fast-slow pleiotropy at an underlying locus). The three other life history QTLs all underlie variation in BSD2; notably, LH5 (the largest at $r^2 = 0.21$) solely affects BSD2 in opposition to the parental difference, while WFM alleles at the two multi-trait QTL clusters (LH2 and LH5) increase BSD2 while decreasing rhizome number and increasing biomass, respectively (Table 2).

For physiological/functional traits, we detected a Mendelian QTL on Chromosome 4 for anthocyanin production on the main
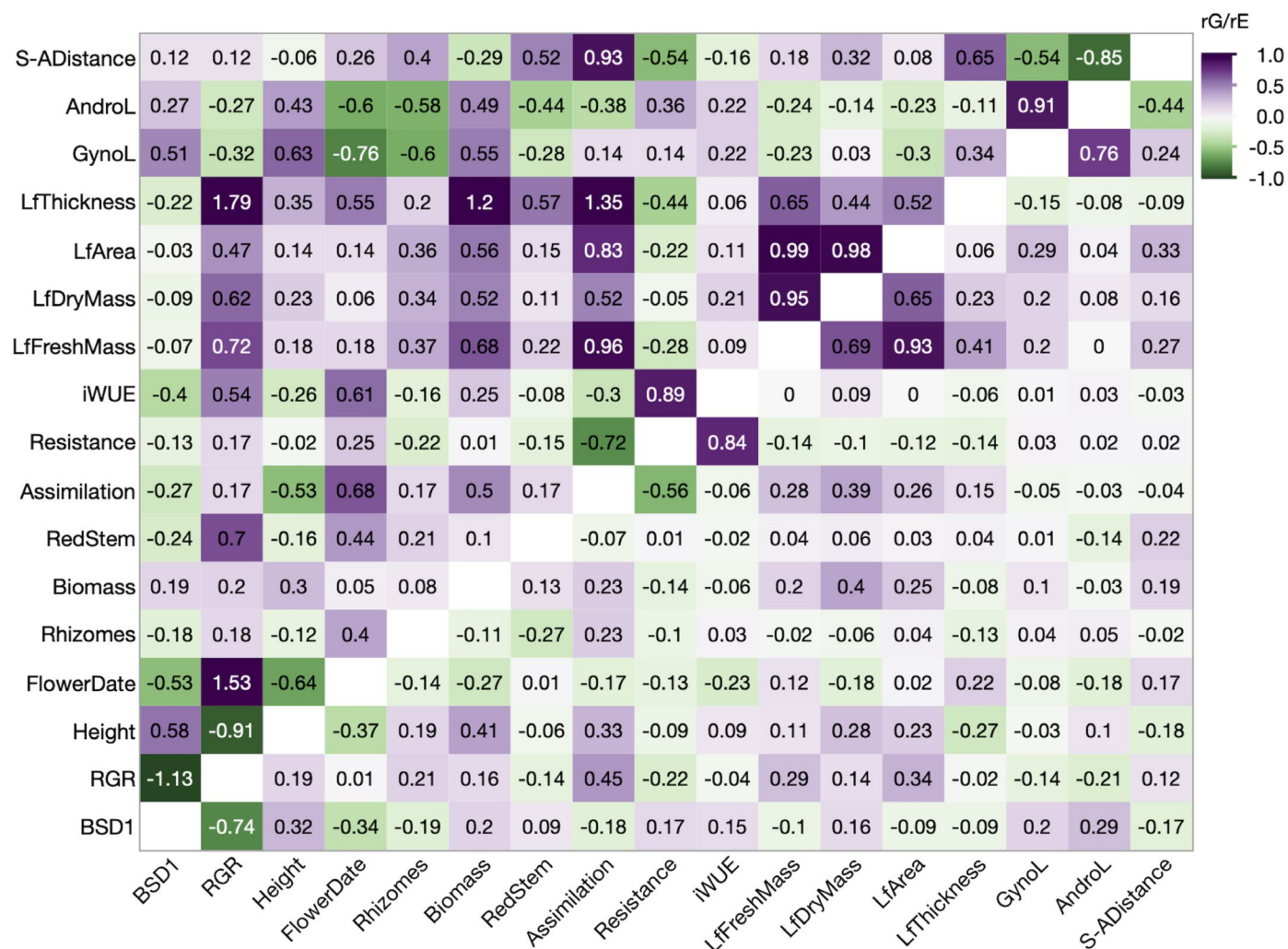
	BSD1	RGR	Height	FlowerDate	Rhizomes	Biomass	RedStem	Assimilation	Resistance	iWUE	LfFreshMass	LfDryMass	LfArea	LfThickness	GynoL	AndroL	S-ADistance
S-ADistance	0.12	0.12	-0.06	0.26	0.4	-0.29	0.52	0.93	-0.54	-0.16	0.18	0.32	0.08	0.65	-0.54	-0.85	
AndroL	0.27	-0.27	0.43	-0.6	-0.58	0.49	-0.44	-0.38	0.36	0.22	-0.24	-0.14	-0.23	-0.11	0.91		-0.44
GynoL	0.51	-0.32	0.63	-0.76	-0.6	0.55	-0.28	0.14	0.14	0.22	-0.23	0.03	-0.3	0.34		0.76	0.24
LfThickness	-0.22	1.79	0.35	0.55	0.2	1.2	0.57	1.35	-0.44	0.06	0.65	0.44	0.52		-0.15	-0.08	-0.09
LfArea	-0.03	0.47	0.14	0.14	0.36	0.56	0.15	0.83	-0.22	0.11	0.99	0.98		0.06	0.29	0.04	0.33
LfDryMass	-0.09	0.62	0.23	0.06	0.34	0.52	0.11	0.52	-0.05	0.21	0.95		0.65	0.23	0.2	0.08	0.16
LfFreshMass	-0.07	0.72	0.18	0.18	0.37	0.68	0.22	0.96	-0.28	0.09		0.69	0.93	0.41	0.2	0	0.27
iWUE	-0.4	0.54	-0.26	0.61	-0.16	0.25	-0.08	-0.3	0.89		0	0.09	0	-0.06	0.01	0.03	-0.03
Resistance	-0.13	0.17	-0.02	0.25	-0.22	0.01	-0.15	-0.72		0.84	-0.14	-0.1	-0.12	-0.14	0.03	0.02	0.02
Assimilation	-0.27	0.17	-0.53	0.68	0.17	0.5	0.17		-0.56	-0.06	0.28	0.39	0.26	0.15	-0.05	-0.03	-0.04
RedStem	-0.24	0.7	-0.16	0.44	0.21	0.1		-0.07	0.01	-0.02	0.04	0.06	0.03	0.04	0.01	-0.14	0.22
Biomass	0.19	0.2	0.3	0.05	0.08		0.13	0.23	-0.14	-0.06	0.2	0.4	0.25	-0.08	0.1	-0.03	0.19
Rhizomes	-0.18	0.18	-0.12	0.4		-0.11	-0.27	0.23	-0.1	0.03	-0.02	-0.06	0.04	-0.13	0.04	0.05	-0.02
FlowerDate	-0.53	1.53	-0.64		-0.14	-0.27	0.01	-0.17	-0.13	-0.23	0.12	-0.18	0.02	0.22	-0.08	-0.18	0.17
Height	0.58	-0.91		-0.37	0.19	0.41	-0.06	0.33	-0.09	0.09	0.11	0.28	0.23	-0.27	-0.03	0.1	-0.18
RGR	-1.13		0.19	0.01	0.21	0.16	-0.14	0.45	-0.22	-0.04	0.29	0.14	0.34	-0.02	-0.14	-0.21	0.12
BSD1		-0.74	0.32	-0.34	-0.19	0.2	0.09	-0.18	0.17	0.15	-0.1	0.16	-0.09	-0.09	0.2	0.29	-0.17

FIGURE 2. Environmental (r_E; below the diagonal) and genetic (r_G; above the diagonal) correlations calculated from parental and hybrid covariances for traits with $H^2 \geq 0.20$. Because r_G is calculated assuming r_E in the non-recombining classes equals r_E in the segregating F_2 hybrids, values can be greater than 1 or < –1, especially when r_E is low or opposite in direction to the F_2 phenotypic covariance.

stem (RedStem4; max LOD = 13.1, p < 0.00001). RedStem4 had additive effects, with heterozygotes (like F_1s) intermediate between CE10 (no anthocyanin flush) and WFM (strong flush). This suggests a simple regulatory switch controlling vegetative anthocyanin production under benign greenhouse growth conditions. We detected no QTLs for the three leaf size traits, despite substantial H^2 (Table 1), or for the low-heritability traits LMA or LDMC. A broad region on Chromosome 1 (LFunct1) was associated with F_2 variation in iWUE, with CE10 alleles recessively increasing water use efficiency. LFunct1 overlaps with a secondary QTL for stomatal resistance (CE10 homozygotes high, as expected from parental difference), but the region had no significant association with photosynthetic rate. Finally, we mapped a tight cluster of QTLs on Chromosome 7 (LFunct7) for photosynthetic assimilation and stomatal resistance (r^2 = 0.19 and 0.21, respectively), as well as leaf thickness (r^2 = 0.16). Because the two gas exchange traits have only H^2 of 0.25-0.43 (i.e., a large fraction of the date-standardized F_2 phenotypic variance is not genetic), this major QTL may be sufficient to explain much of their between-population genetic differentiation. Indeed, the two

homozygous F_2 genotypes at LFunct7 are more differentiated than the parental means (both standardized and unstandardized values).

Floral traits associated with mating system mapped to QTL clusters on four chromosomes. Rep1 affected both androecium length (r^2 = 0.21, WFM larger) and stigma-anther separation (r^2 = 0.16, WFM smaller), while Rep7 had similar effects in the opposite direction (androecium length: r^2 = 0.18, WFM smaller; stigma-anther separation: r^2 = 0.14, WFM larger). Rep6 affected gynoecium and androecium length in concert (r^2 = 0.16 and 0.17, respectively; CE10 homozygote shorter for both), so had no effect on stigma-anther separation. Rep4 was strongly associated with stigma-anther separation (r^2 = 0.25), but not (significantly) with the length of male or female reproductive organs separately. The allelic effects of this major QTL go in the opposite direction from the expectation from the parental difference. That is, WFM homozygotes (N = 16, mean = 2.44) have much greater stigma-anther separation than CE10 homozygotes (N = 26, mean = 0.53), with heterozygotes intermediate. The variable directionality and dominance of individual floral QTL effects in hybrids likely contributes to the
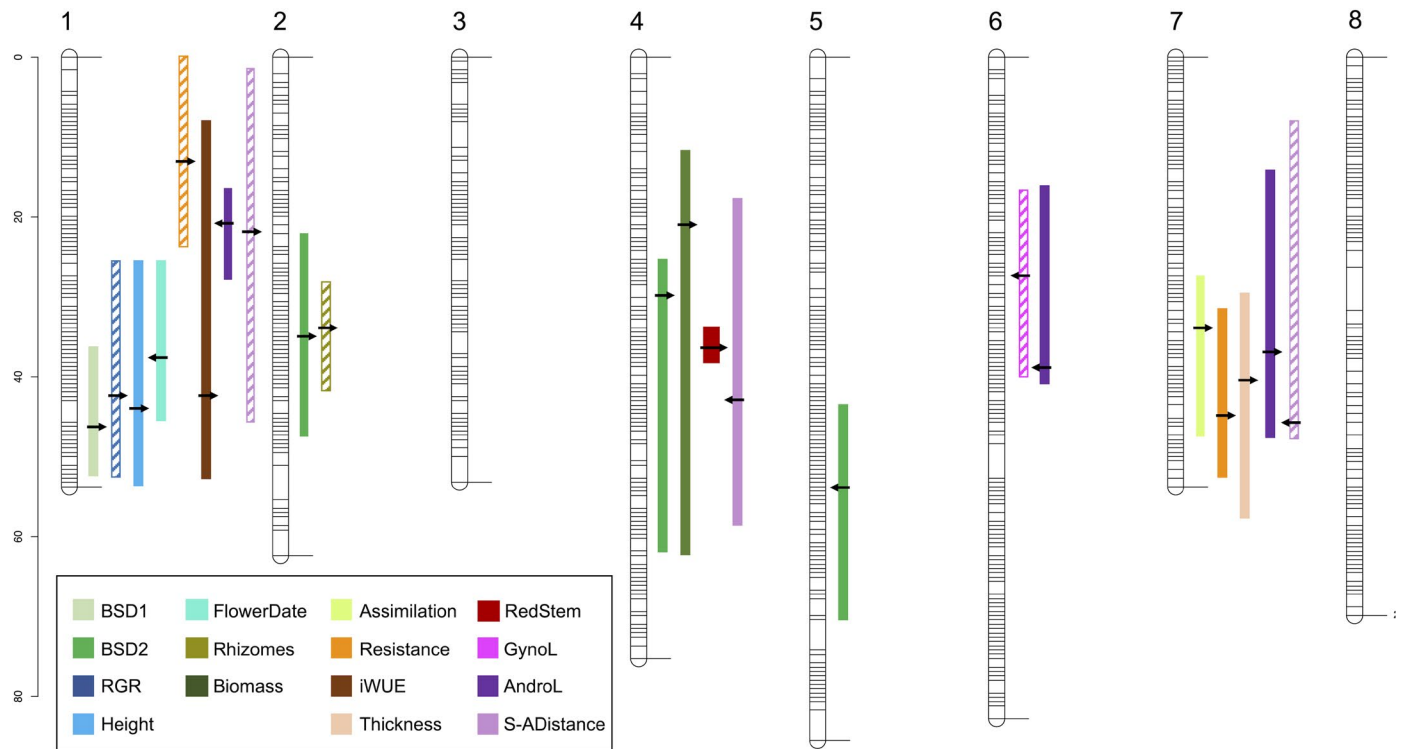
FIGURE 3. Quantitative trait loci (QTLs) for life history, leaf function, and floral traits in intra-population *Mimulus cardinalis* hybrids, mapped onto the eight linkage groups/chromosomes. Scale at left is centiMorgans (cM), and the positions of 720 linkage-informative gene-based markers are shown on linkage groups. Colored bars show the 1.5 LOD drop confidence interval around each peak (solid: primary QTLs at genome-wide α = 0.05 LOD thresholds 3.40–3.78, depending on trait; hashed: secondary QTLs at genome-wide α = 0.15, LOD > 3.02–3.14, depending on trait). Arrows show the location of QTL peaks, with the arrowhead pointing right if the direction of allelic effects matches the expectation from parental means. The width of the QTL bars reflects the PVE (narrow: 0.14 to 0.25, wide: >0.25). See Table 2 for QTL groupings and effect sizes.

unexpectedly low stigma-anther distances of F_1s (Table 1). All three stigma-anther separation QTLs remained significant in a model with all included, but we did not have sufficient F_2 numbers to scan for epistatic interactions.

DISCUSSION

Multi-trait divergence between populations reflects life-history adaptation to local soil moisture regimes

The transition between perenniality and annuality is one of the most common in flowering plants, changing the context for selection on numerous other traits, and yet remains poorly understood from both ecological and genetic perspectives (Lundgren and Marais, 2020). Although *M. cardinalis* is generally considered to be a perennial species, plants in Southern California populations often do not survive summer dry-down (Sheth and Angert, 2018), particularly during severe drought periods (A. Angert, personal observation). In particular, our focal Southern population (WFM) had the lowest year-to-year survival rate of >30 populations tracked, and low survival was not ecologically compensated for by seedling recruitment (Sheth and Angert, 2018). Despite this ongoing demographic challenge, Southern populations appear relatively well-adapted to highly variable summer water regimes along a drought-avoidance axis (Muir and Angert, 2017; Sheth and Angert, 2018). Our results demonstrate that they are also morphologically annualized, with fast early growth, greater biomass and height, and no rhizome production under greenhouse conditions. Low rhizome production newly indicates a genetic loss of perenniality, paralleling a widespread life-history polymorphism segregating across soil moisture regimes in the yellow monkeyflower (*M. guttatus*) (Lowry and Willis, 2010). These heritable differences in growth form suggest that southern populations have responded evolutionarily to climate (see also Sheth, 2016) and have the potential to share adaptive variation with northern populations experiencing increased drought (Paul et al., 2011).

The annualized life-history of WFM Southern *M. cardinalis* is accompanied by genetic differences in leaf physiological traits consistent with an adaptive drought-escape strategy (Table 1). Several trends parallel expectations for a fast-slow axis of LES variation, i.e., initially fast-growing WFM plants appear more "resource-acquisitive" in that they have relatively high area-standardized photosynthetic rates, plus lower stomatal resistance and water use efficiency (Table 1). However, these physiological differences are positively associated with leaf thickness differences between populations. Both LMA and leaf thickness are greater in WFM plants, but LMDC is lower (Table 1), suggesting that WFM's higher fresh mass reflects disproportionately increased water content per unit area (i.e., succulence or thickness) rather than increased cell density or investment in cell wall. Although not consistent with LES predictions (Wright et al., 2004; Poorter et al., 2009), this combination of

TABLE 2. Quantitative trait loci (QTLs; alternating white and gray), grouped by trait category and chromosome if overlapping within a category, with peak cM position, LOD score (italicized if only significant at the secondary α = 0.15 level) , r² (or PVE; percent of F_2 variance explained), and QTL additive (*a* = WFM homozygote mean minus the midparent value) and dominance (*d* = heterozygote mean minus the midparent value) effect estimates for each trait. Values of *a* are negative when the WFM homozygote has the lower trait value and *a* and *d* share their sign when the WFM allele is (partially) dominant. The value of *a* is bolded if the effect of the QTL is in the direction expected from the parental difference and italicized if opposite to the parental difference.

QTL	Trait	LG	cM	LOD	PVE/r²	*a*	*d*
LH1	BSD1	1	46.25	4.55	0.20	**0.22**	0.33
LH1	RGR	1	42.48	*3.40*	0.16	−0.04	−0.04
LH1	Height	1	44.00	3.60	0.16	**13.83**	8.66
LH1	Days to flower	1	38.18	4.01	0.18	*−2.34*	−1.14
LFunct1	Resistance	1	12.91	*3.25*	0.15	−0.23	−0.49
LFunct1	iWUE	1	42.48	4.03	0.18	−3.99	−3.06
Rep1	Androecium length	1	20.01	4.70	0.21	*1.45*	−0.45
Rep1	Stigma-anther separation	1	22.05	*3.42*	0.16	−0.69	0.37
LH2	BSD2	2	34.95	*3.61*	0.16	0.42	−0.10
LH2	Rhizomes	2	33.88	*3.06*	0.14	−1.28	−0.04
LH4	BSD2	4	30.00	3.79	0.17	0.46	−0.06
LH4	Biomass	4	20.97	*3.69*	0.17	**1.18**	−0.88
RedStem4	Stem anthocyanin	4	36.57	13.10	0.48	**0.99**	−0.18
Rep4	Stigma-anther separation	4	43.02	5.82	0.25	*0.95*	−0.45
LH5	BSD2	5	54.31	4.83	0.21	−0.46	0.06
Rep6	Gynoecium length	6	27.42	*3.51*	0.16	*1.03*	0.63
Rep6	Androecium length	6	39.25	3.75	0.17	*1.31*	0.87
LFunct7	Assimilation (A_area)	7	34.00	4.24	0.19	**1.27**	0.46
LFunct7	Resistance	7	45.00	4.79	0.21	**−0.70**	−0.32
LFunct7	Leaf thickness	7	40.33	3.98	0.16	**12.96**	0.32
Rep7	Androecium length	7	37.10	3.95	0.18	**−1.05**	0.85
Rep7	Stigma-anther separation	7	46.24	*3.10*	0.14	*0.81*	0.18

high photosynthetic assimilation rate with relatively high LMA in the more arid and seasonal climate parallels patterns in similar herbaceous taxa (Mason and Donovan, 2015). However, even within herbs, leaf functional traits may experience different selection from drought (e.g., for tolerance vs. escape) depending on life history. In perennial *Silene latifolia* Poir. [Caryophyllaceae], xeric populations tended to have thicker leaves but also slower growth trajectories compared to mesic populations, suggesting tolerance (Delph, 2019). In contrast, increased leaf succulence (same as our thickness) and early flowering were significantly associated with aridity across replicate clines of annual *M. guttatus* (Kooyers et al., 2015), parallel to annualized *M. cardinalis*. Along with other common garden studies (Muir et al., 2017; Ahrens et al., 2020), this work suggests that unexpected (from between-species LES patterns) associations among leaf functional traits may reflect locally adapted genetic variation, as well as plasticity in individual traits (Anderegg et al., 2018).

The evolution of annuality in ephemeral habitats may often precipitate selection on phenological and floral traits associated with rapid reproduction (reviewed in Barrett et al., 1996; Gaudinier and Blackman, 2020). Paralleling latitudinal clines in previous

studies of *M. cardinalis* (Muir and Angert, 2017), our Southern WFM accession flowers slightly later than the Sierran CE10 line. Later flowering may be non-intuitive, given WFM's otherwise "fast" life-history, but annualized southern populations may experience a longer interval between germination and peak pollinator activity vs. perennial Sierran populations bounded by last spring and first fall freezes. Intriguingly, Southern *M. cardinalis* populations are also uniquely responsive to artificial selection on flowering time (Sheth, 2016), suggesting that spatial and temporal variation in soil moisture may maintain local genetic variation for this trait. Greater environmental unpredictability likely also accounts for the smaller flower size and reduced stigma-anther separation (classic selfing syndrome traits; Sicard and Lenhard, 2011) of WFM *M. cardinalis*. Southern *M. cardinalis* co-occurs (and hybridizes) with the tiny-flowered selfer *M. parishii* Greene (Fishman et al., 2015) and its more quantitative shifts in floral traits may reflect shared environmental selection for self-fertilization as reproductive assurance (as in *M. guttatus*, see Fishman and Willis, 2008; Bodbyl Roels and Kelly, 2011). Reduced stigma-anther separation (relative to Sierran plants) has also been reported for *M. cardinalis* collected near the northern range limit (Hazle and Hilliker, 2005), suggesting selection for selfing at both range edges. However, the biotic communities in each region, abiotic factors selecting on correlated corolla traits, or drift/inbreeding may also contribute to floral variation, and more work will be necessary to characterize *M. cardinalis* mating systems in the wild.

Composite functional traits often exhibit transgressive means and low heritability in hybrids, suggesting independent genetic bases for the underlying components

Our experimental hybrids display two patterns that complicate evolutionary predictions about composite leaf functional traits often used as ecological proxies. First, independent assortment and dominance of component traits may cause composite traits in F_1 hybrids to be more extreme that either parental genotype (over- or underdominance, respectively) (Rieseberg et al., 2011; Thompson et al., 2021). In our cross, the low photosynthetic rates of the CE10 parent are coupled with the low stomatal resistance of the WFM parent in F_1s, resulting in transgressively low hybrid iWUE; the floral composite trait of stigma-anther separation is similarly underdominant (Table1). Such mis-matched composite phenotypes may reduce the fitness of hybrids between divergent populations, slowing evolutionary rescue under contemporary climate change (Thompson et al., 2021). Second, later-generation hybrids may exhibit low heritability or transgressive segregation because genes underlying component traits sort into novel combinations (Rieseberg et al., 1999), potentially with epistatic interactions (Muir and Moyle, 2009). In this study, two composite LES traits (LMA and LDMC) exhibited low heritability (<0.10), despite substantial parental differentiation and high heritability of the underlying components (Table 1). Low heritability and/or transgressive inheritance in hybrids raise the question of whether composite traits often used as ecological proxies, such as LMA, generally diverge as direct targets of selection or as by-products of selection on component traits. The answer likely depends on the particular composite trait and its genetic architecture; for example, stigma-anther separation rapidly responds to selection for increased autogamous self-fertilization (Bodbyl Roels and Kelly, 2011). However, our results suggest that separating the individual components of composite functional traits may be key to

predicting their evolutionary trajectories, especially in novel genetic backgrounds and environments.

The first intraspecific genetic map for *Mimulus* section *Erythranthe* provides a key resource for ecological and comparative genomics in this model system

Genetic mapping in *Mimulus* sect. *Erythranthe* (Spach) Greene has focused on inter-specific crosses (Bradshaw et al., 1995; Fishman et al., 2013; 2015) and/or narrow genetic introgressions containing induced mutations or candidate loci for species differences (Yuan et al. 2013a, 2013b). However, section *Erythranthe* species' pairs are distinguished by chromosomal inversions that suppress recombination and translocations that cause sterility in F_1 hybrids (Fishman et al., 2013; Stathos and Fishman, 2014). Thus, inter-specific maps involving *M. cardinalis* only resolve 6 or 7 linkage groups (Fishman et al., 2013, 2014, 2015), confounding the genetics of adaptive differentiation with processes of chromosomal divergence and speciation. Our gene-anchored intraspecific map cleanly resolves the expected 8 section *Erythranthe* chromosomes, advancing study of the comparative evolutionary genetics of trait divergence across *Mimulus*. For example, the Mendelian RedStem4 QTL occurs in the center of *M. cardinalis* Chromosome 4, which is syntenic with *M. guttatus* LG8 (Fishman et al., 2014). A cluster of three R2R3 MYB genes on LG8 underlies floral and vegetative anthocyanin polymorphisms in the *M. guttatus* species complex (Cooley et al., 2011; Lowry et al., 2012), and the syntenic region also controls corolla anthocyanin patterning traits in section *Erythranthe* (Yuan et al., 2014). This evidence of a conserved regulatory basis for vegetative anthocyanins encourages comparative analyses of stress tolerance and pigmentation. Further, within-*M. cardinalis* genetic mapping of diverse traits provides a framework for future ecological genomics using approaches complicated by linkage disequilibrium (e.g., genome-wide association mapping) or blind to traits (e.g., F_{ST} outlier analysis).

Multi-trait QTL clusters suggest modular adaptation, but only weak co-ordination between fast-slow life history and leaf functional traits

The molecular genetic basis of perennial to annual transitions remains surprisingly opaque across herbaceous plants (reviewed in Friedman and Rubin, 2015), and QTL analyses are an important step toward understanding co-ordinated life history evolution. Our QTL analyses identified multi-trait QTL clusters consistent with modular evolution of early and late growth. For example, LH1 had parallel effects on early growth (BSD1), flowering time, and height (Table 2; Fig. 3), resembling the major DIV1 QTL in yellow monkeyflowers (Hall et al., 2006; Lowry and Willis, 2010; Friedman et al., 2015); however, LH1 had no detectable effects on rhizome production or biomass, key traits for the perennial-annual transition. Three additional QTL clusters (LH2, LH4, and LH6) influenced BSD2, with little or no effect on BSD1. WFM alleles in the LH2 and LH4 regions increased BSD2 (counter to the parental difference), while also decreasing rhizome production (LH2) and increasing final biomass (LH4). This pattern suggests strong modularity of early and late growth, with the former genetically associated with flowering phenology and the latter mediating total aboveground biomass and potentially trading off against rhizome production. LH1 is also the best

(but still modest) candidate for co-ordination of life history and leaf functional QTLs, as it overlaps with a QTL affecting iWUE through elevated stomatal resistance in Sierran (CE10) homozygotes. LH1/LFunct1 effects are consistent with fast-slow axis predictions, with "slow" CE10 alleles relatively resource-conservative in terms of leaf traits (high iWUE and low stomatal resistance). However, the iWUE QTL is extremely broad (Fig. 3) and co-localization of iWUE and RGR peaks may not be due to tight linkage or pleiotropy.

Beyond the partial overlap of LH1 and LFunct1, there is scant evidence that leaf physiology and life history/growth are genetically associated either genome-wide (Fig. 2) or at the individual locus level (Table 2, Fig. 3). Instead, the coordinated effects of our largest leaf functional QTL (LFunct7) reveal intriguing genetic linkages between leaf structure and physiological traits ecologically associated with life history and climatic adaptation. The WFM allele at LFunct7 additively increases photosynthetic rate (A_{area}) and leaf thickness while reducing stomatal resistance (r_{sw}) enough to explain the population difference in photosynthetic traits. Plants with thick or succulent leaves are generally considered to be on the slow/resource-conservative end of the LES (Wright et al., 2004) and genetic associations between leaf thickness and slower growth have been interpreted as evidence of a leaf-level tradeoff (Coneva et al., 2017; Coneva and Chitwood, 2018). In contrast, southern *M. cardinalis* plants (WFM) plants appear to support rapid early growth with unlinked variation generating high photosynthetic rates and relatively thick leaves. Thus, the co-ordination of physiological and life-history fast-slow axes seen at broad scales (Adler et al., 2014; Salguero-Gómez, 2017) does not derive (at least in *Mimulus*) from widespread genetic or resource constraints at the leaf-level.

Furthermore, co-mapping of thickness and gas exchange traits suggests that wet mass/area may be a better predictor of area-standardized photosynthetic capacity (and a fast life history) than LMA (dry mass/area) in high-light-adapted taxa (Vile et al., 2005). A strong locus-level tradeoff between photosynthetic rate and resistance could simply reflect pleiotropic effects of stomatal density or regulation, with WFM exchanging more CO_2 and losing more H_2O for a given leaf area. However, *M. cardinalis* have stomata on both leaf surfaces (i.e., are amphistomatous) and our focal populations do not differ in stomatal density (202 mm^{-2} for CE10 versus 200 mm^2 for WFM; C. Muir, unpublished data). Amphistomy is expected in high-light taxa such as *Mimulus*; by allowing greater delivery of CO_2 to mesophyll cells for a given leaf thickness, it may enhance photosynthetic efficiency when light is not limiting (Mott et al., 2006; Muir, 2019). In amphistomatous taxa, the co-localization of gas exchange and leaf thickness QTLs suggests an alternative mechanism. Thicker leaves generally have taller mesophyll palisade cells and greater photosynthetic efficiency (Terashima et al., 2001), and LFunct7 could affect all three through structural changes to the mesophyll layer. In *Populus* [Salicaceae], trees from shorter growing seasons have leaves with higher photosynthesis rates genetically associated with anatomical differences increasing the exposure of mesophyll cell surface area to airspace (Soolanayakanahally et al., 2009; Milla-Moreno et al., 2016). Our mapping of LFunct7 in the light-loving herb *M. cardinalis*, where greater leaf thickness is genetically associated with a fast, resource-acquisitive, drought-escape strategy, suggests this may be a common physiological mechanism under simple genetic control.

Caveats and limitations

Despite power to detect major QTLs and rule out joint (major) effects of a given genomic region on multiple traits, our small F_2 mapping population limits inference about the genetic architecture of any individual trait. Effect sizes of detected QTLs are likely upwardly-biased (Beavis, 1994), and we detected no primary QTLs for several substantially heritable traits (e.g., leaf fresh and dry mass, gynoecium length). Thus, numerous additional small-effect loci undoubtedly influence all heritable traits. We also had low power to distinguish weak linkage from adaptively suppressed recombination (like DIV1; Lowry and Willis, 2010) or pleiotropy, while our two-step approach to identifying coincident QTL clusters risks over-detection of multi-trait QTLs. However, only two additional QTLs (one for stigma-anther separation, one for leaf thickness) would have been mapped in an initial scan at the lower secondary threshold. In addition, our rejection of a joint genetic basis for fast-slow physiology and life history axes is strongly corroborated by the absence of genome-wide genetic correlations between leaf functional traits and BSD1 (early growth), flowering time, or rhizome production. Finally, the line-cross approach samples limited *M. cardinalis* variation and risks confounding inbreeding depression specific to our lines with the genetic architecture of adaptation. However, only six of 22 QTLs had effects opposite to those expected and, for some (e.g., the flowering time effects of LH1) the locus-level effects were instead consistent with expectations of the fast-slow life history axis. Furthermore, parental differences in physiology parallel trends across the species' range (Muir and Angert, 2017), suggesting that we have primarily captured the genetics of *M. cardinalis* adaptation across climatic gradients.

CONCLUSIONS

Understanding the evolutionary past and future potential of plant adaptation requires knowledge of the genetic mechanisms underlying differentiation in individual traits and correlated trait syndromes. Our genetic characterization of life-history, physiological, and floral divergence between scarlet monkeyflower (*Mimulus cardinalis*) populations adapted to distinct seasonal habitats provide an important step toward understanding the correlated trait syndromes in this ecological model species. First, we find that intra-specific differentiation between the parental populations (partly) parallels coordinated shifts in life-history, mating system, and physiology seen at larger taxonomic scales. Second, we demonstrated high heritability for many individual traits, as well as genetic correlations potentially contributing to functional associations, but found low heritability for several key traits from the leaf economics spectrum (e.g., LMA). Third, by constructing a high-density, gene-based intraspecific linkage map, we identified QTLs for several traits of interest, most notably a Mendelian locus controlling vegetative anthocyanin and separate multi-trait QTLs underlying early growth and flowering, late growth and asexual reproduction, and leaf thickness and gas exchange traits, respectively. The leaf functional trait QTL argues for more detailed studies of leaf anatomy variation across *Mimulus* populations, and broadly across herbaceous plants. Overall, these findings suggest that traits associated with a drought avoidance syndrome in annualized *Mimulus cardinalis* have a modular genetic basis, allowing for independent evolution of the different components; however, functional coordination of both life history and leaf physiological traits may allow rapid adaptation to novel climatic conditions across the species' range.

DATA AVAILABILITY

The sequencing data are available on the NCBI Sequence Read Archive under BioProject PRJNA684598 (accessions SAMN17062083-SAMN17062176), and the phenotype-genotype data have been archived at the Dryad Digital Repository: doi.org/10.5061/dryad.m0cfxpp2q (Nelson et al., 2021a).

LITERATURE CITED

Ackerly, D. D., S. A. Dudley, S. E. Sultan, J. Schmitt, J. S. Coleman, C. R. Linder, D. R. Sandquist, et al. 2000. The evolution of plant ecophysiological traits: Recent advances and future directions. *Bioscience* 50: 979–995.

Adler, P. B., R. Salguero-Gómez, A. Compagnoni, J. S. Hsu, J. Ray-Mukherjee, C. Mbeau-Ache, and M. Franco. 2014. Functional traits explain variation in plant life history strategies. *Proceedings of the National Academy of Sciences, USA* 111: 740–745.

Agrawal, A. A. 2020. A scale-dependent framework for trade-offs, syndromes, and specialization in organismal biology. *Ecology* 101: e02924.

Ahrens, C. W., M. E. Andrew, R. A. Mazanec, K. X. Ruthrof, G. Challis, G. Hardy, M. Byrne, et al. 2020. Plant functional traits differ in adaptability and are predicted to be differentially affected by climate change. *Ecology and Evolution* 10: 232–248.

Anderegg, L. D. L., L. T. Berner, G. Badgley, M. L. Sethi, B. E. Law, and J. HilleRisLambers. 2018. Within-species patterns challenge our understanding of the leaf economics spectrum. *Ecology Letters* 21: 734–744.

Angert, A. L. 2006. Growth and leaf physiology of monkeyflowers with different altitude Ranges. *Oecologia* 148: 183–194.

Angert, A. L., S. Kimball, M. Peterson, T. E. Huxman, and D. L. Venable. 2014. Phenotypic constraints and community structure: Linking trade-offs within and among species. *Evolution* 68: 3149–3165.

Angert, A. L., S. N. Sheth, and J. R. Paul. 2011. Incorporating population-level variation in thermal performance into predictions of geographic range shifts. *Integrative and Comparative Biology* 51: 733–750.

Barker, W., G. Nesom, P. Beardsley, and N. S. Fraga. 2012. A taxonomic conspectus of Phrymaceae: A narrowed circumscription for *Mimulus,* new and resurrected genera, and new names and combinations. *Phytoneuron* 39: 1–60.

Barrett, S. C. H. 2002. The evolution of plant sexual diversity. *Nature Reviews Genetics* 3: 274–284.

Barrett, S. C. H., L. D. Harder, and A. C. Worley. 1996. The comparative biology of pollination and mating in flowering plants. *Philosophical Transactions of the Royal Society, B, Biological Sciences* 351: 1271–1280.

Beavis, W. D. 1994. The power and deceit of QTL experiments: Lessons from comparative QTL studies. *In* D.B. Wilkinson [ed.], Proceedings of the 49th Annual Corn and Sorghum Industry Research Conference in Chicago, Illinois, 250–266. American Seed Trade Association, Washington, District of Columbia, USA.

Bodbyl Roels, S. A., and J. K. Kelly. 2011. Rapid evolution caused by pollinator loss in *Mimulus guttatus*. *Evolution* 65: 2541–2552.

Bolger, A. M., M. Lohse, and B. Usadel. 2014. Trimmomatic: A flexible trimmer for Illumina sequence data. *Bioinformatics* 30: 2114–2120.

Bradshaw, H. D., Jr., and D. W. Schemske. 2003. Allele substitution at a flower colour locus produces a pollinator shift in monkeyflowers. *Nature* 426: 176–178.

Bradshaw, H. D., Jr., S. M. Wilbert, K. G. Otto, and D. W. Schemske. 1995. Genetic mapping of floral traits associated with reproductive isolation in monkeyflowers (*Mimulus*). *Nature* 376: 762–765.

Broman, K. W., H. Wu, S. Sen, and G. A. Churchill. 2003. R/qtl: QTL mapping in experimental crosses. *Bioinformatics* 19: 889–890.

Coneva, V., and D. H. Chitwood. 2018. Genetic and developmental basis for increased leaf thickness in the *Arabidopsis* Cvi ecotype. *Frontiers in Plant Science* 9: 322.

Coneva, V., M. H. Frank, M.A. de L. Balaguer, M. Li, R. Sozzani, and D.H. Chitwood. 2017. Genetic architecture and molecular networks underlying leaf thickness in desert-adapted tomato *Solanum pennellii*. *Plant Physiology* 175: 376–391.

Cooley, A. M., J. L. Modliszewski, M. L. Rommel, and J. H. Willis. 2011. Gene duplication in *Mimulus* underlies parallel floral evolution via independent trans-regulatory changes. *Current Biology* 21: 700–704.

Delph, L. F. 2019. Water availability drives population divergence and sex-specific responses in a dioecious plant. *American Journal of Botany* 106: 1346–1355.

Derroire, G., J. S. Powers, C. M. Hulshof, L. E. C. Varela, and J. R. Healey. 2018. Contrasting patterns of leaf trait variation among and within species during tropical dry forest succession in Costa Rica. *Scientific Reports* 8: 285.

Díaz, S., J. Kattge, J. H. C. Cornelissen, I. J. Wright, S. Lavorel, S. Dray, B. Reu, et al. 2016. The global spectrum of plant form and function. *Nature* 529: 167–171.

Donovan, L. A., H. Maherali, C. M. Caruso, H. Huber, and H. De Kroon. 2011. The evolution of the worldwide leaf economics spectrum. *Trends in Ecology & Evolution* 26: 88–95.

Fajardo, A., and A. Siefert. 2018. Intraspecific trait variation and the leaf economics spectrum across resource gradients and levels of organization. *Ecology* 99: 1024–1030.

Fishman, L., P. Beardsley, A. Stathos, C. F. Williams, and J. P. Hill. 2015. The genetic architecture of traits associated with the evolution of self-pollination in *Mimulus*. *New Phytologist* 205: 907–917.

Fishman, L., A. J. Kelly, and J. H. Willis. 2002. Minor quantitative trait loci underlie floral traits associated with mating system divergence in *Mimulus*. *Evolution* 56: 2138–2155.

Fishman, L., and M. McIntosh. 2019. Standard deviations: The biological bases of transmission ratio distortion. *Annual Review of Genetics* 53: 347–372.

Fishman, L., A. Stathos, P. Beardsley, C. F. Williams, and J. P. Hill. 2013. Chromosomal rearrangements and the genetics of reproductive barriers in *Mimulus* (monkeyflowers). *Evolution* 67: 2547–2560.

Fishman, L., and J. H. Willis. 2008. Pollen limitation and natural selection on floral characters in the yellow monkeyflower, *Mimulus guttatus*. *New Phytologist* 177: 802–810.

Fishman, L., J. H. Willis, C. A. Wu, and Y. W. Lee. 2014. Comparative linkage maps suggest that fission, not polyploidy, underlies near-doubling of chromosome number within monkeyflowers (*Mimulus*; Phrymaceae). *Heredity* 112: 562–568.

Friedman, J., and M. J. Rubin. 2015. All in good time: Understanding annual and perennial strategies in plants. *American Journal of Botany* 102: 497–499.

Friedman, J., A. D. Twyford, J. H. Willis, and B. K. Blackman. 2015. The extent and genetic basis of phenotypic divergence in life history traits in *Mimulus guttatus*. *Molecular Ecology* 24: 111–122.

Gaudinier, A., and B. K. Blackman. 2020. Evolutionary processes from the perspective of flowering time diversity. *New Phytologist* 225: 1883–1898.

Geber, M. A., and L. R. Griffen. 2003. Inheritance and natural selection on functional traits. *International Journal of Plant Sciences* 164 (Suppl. 3): S21–S42.

Guilherme Pereira, C., and D.L. des Marais. 2020. The genetic basis of plant functional traits and the evolution of plant-environment interactions. *International Journal of Plant Sciences* 181: 56–74.

Hall, M. C., C. J. Basten, and J. H. Willis. 2006. Pleiotropic quantitative trait loci contribute to population divergence in traits associated with life-history variation in *Mimulus guttatus*. *Genetics* 172: 1829–1844.

Hazle, T., and J. C. Hilliker. 2005. Floral ontogeny and allometry of *Mimulus cardinalis*: Interpopulational variation and traits of the hummingbird-pollination syndrome. *International Journal of Plant Sciences* 166: 61–83.

Hiesey, W., M. Nobs, and O. Bjorkman. 1971. Experimental studies on the nature of species: 5. Biosystematics, genetics and physiological ecology of the *Erythranthe* section of *Mimulus*. Carnegie Institution of Washington, Washington, District of Columbia, USA.

Ivey, C. T., L. S. Dudley, A. A. Hove, S. K. Emms, and S. J. Mazer. 2016. Outcrossing and photosynthetic rates vary independently within two *Clarkia* species: Implications for the joint evolution of drought escape physiology and mating system. *Annals of Botany* 118: 897–905.

Ji, W., S. E. LaZerte, M. J. Waterway, and M. J. Lechowicz. 2020. Functional ecology of congeneric variation in the leaf economics spectrum. *New Phytologist* 225: 196–208.

Kimball, S., J. R. Gremer, T. E. Huxman, D. L. Venable, and A. L. Angert. 2013. Phenotypic selection favors missing trait combinations in coexisting annual plants. *American Naturalist* 182: 191–207.

Kooyers, N. J., A. B. Greenlee, J. M. Colicchio, M. Oh, and B. K. Blackman. 2015. Replicate altitudinal clines reveal that evolutionary flexibility underlies adaptation to drought stress in annual *Mimulus guttatus*. *New Phytologist* 206: 152–165.

Li, H., and R. Durbin. 2009. Fast and accurate short read alignment with Burrows-Wheeler transform. *Bioinformatics* 25: 1754–1760.

Li, H., B. Handsaker, A. Wysoker, T. Fennell, J. Ruan, N. Homer, G. Marth, et al. 2009. The Sequence Alignment/Map format and SAMtools. *Bioinformatics* 25: 2078–2079.

Lowry, D. B., C. C. Sheng, J. R. Lasky, and J. H. Willis. 2012. Five anthocyanin polymorphisms are associated with an R2R3-MYB cluster in *Mimulus guttatus* (Phrymaceae). *American Journal of Botany* 99: 82–91.

Lowry, D. B., J. M. Sobel, A. L. Angert, T.-L. Ashman, R. L. Baker, B. K. Blackman, Y. Brandvain, et al. 2019. The case for the continued use of the genus name *Mimulus* for all monkeyflowers. *Taxon* 68: 617–623.

Lowry, D. B., and J. H. Willis. 2010. A widespread chromosomal inversion polymorphism contributes to a major life-history transition, local adaptation, and reproductive isolation. *PLoS Biology* 8: e1000500.

Lundgren, M. R., and D.L. des Marais. 2020. Life history variation as a model for understanding trade-offs in plant-environment interactions. *Current Biology* 30: R180–R189.

Martínez-Berdeja, A., M. C. Stitzer, M. A. Taylor, M. Okada, E. Ezcurra, D. E. Runcie, and J. Schmitt. 2020. Functional variants of DOG1 control seed chilling responses and variation in seasonal life-history strategies in *Arabidopsis thaliana*. *Proceedings of the National Academy of Sciences, USA* 117: 2526–2534.

Mason, C. M., and L. A. Donovan. 2015. Evolution of the leaf economics spectrum in herbs: Evidence from environmental divergences in leaf physiology across *Helianthus* (Asteraceae). *Evolution* 69: 2705–2720.

Mazer, S. J., L. S. Dudley, A. A. Hove, S. K. Emms, and A. S. Verhoeven. 2010. Physiological performance in *Clarkia* sister taxa with contrasting mating systems: Do early-flowering autogamous taxa avoid water stress relative to their pollinator-dependent counterparts? *International Journal of Plant Sciences* 171: 1029–1047.

McKenna, A., M. Hanna, E. Banks, A. Sivachenko, K. Cibulskis, A. Kernytsky, K. Garimella, et al. 2010. The genome analysis toolkit: A MapReduce framework for analyzing next-generation DNA sequencing data. *Genome Research* 20: 1297–1303.

Meyer, M., and M. Kircher. 2010. Illumina sequencing library preparation for highly multiplexed target capture and sequencing. *Cold Spring Harbor Protocols* 2010(6): pdb.prot5448–pdb.prot5448.

Milla-Moreno, E. A., A. D. McKown, R. D. Guy, and R. Y. Soolanayakanahally. 2016. Leaf mass per area predicts palisade structural properties linked to mesophyll conductance in balsam poplar (*Populus balsamifera* L.). *Botany* 94: 225–239.

Mott, K. A., A. C. Gibson, and J. W. O'Leary. 2006. The adaptive significance of amphistomatic leaves. *Plant, Cell & Environment* 5: 455–460.

Muir, C. D. 2019. Is amphistomy an adaptation to high light? Optimality models of stomatal traits along light gradients. *Integrative and Comparative Biology* 59: 571–584.

Muir, C. D., and A. L. Angert. 2017. Grow with the flow: A latitudinal cline in physiology is associated with more variable precipitation in *Erythranthe cardinalis*. *Journal of Ecology* 30: 2189–2203.

Muir, C. D., M. À. Conesa, E. J. Roldán, A. Molins, and J. Galmés. 2017. Weak coordination between leaf structure and function among closely related tomato species. *New Phytologist* 213: 1642–1653.

Muir, C. D., and L. C. Moyle. 2009. Antagonistic epistasis for ecophysiological trait differences between *Solanum* species. *New Phytologist* 183: 789–802.

Muir, C. D., J. B. Pease, and L. C. Moyle. 2014. Quantitative genetic analysis indicates natural selection on leaf phenotypes across wild tomato species (*Solanum* sect. *Lycopersicon*; Solanaceae). *Genetics* 198: 1629–1643.

Nelson, T. C., C. D. Muir, A. M. Stathos, D. D. Vanderpool, K. Anderson, A. L. Angert, and L. Fishman. 2021a. Data from: Quantitative trait locus mapping reveals an independent genetic basis for joint divergence in leaf function, life-history, and floral traits between scarlet monkeyflower (*Mimulus cardinalis*) populations. *Dryad Digital Repository*. https://doi.org/10.5061/dryad.m0cfxpp2q.

Nelson, T. C., A. M. Stathos, D. D. Vanderpool, F. R. Finseth, Y.-W. Yuan, and L. Fishman. 2021b. Ancient and recent introgression shape the evolutionary history of pollinator adaptation and speciation in a model monkeyflower radiation (*Mimulus* section *Erythranthe*). *PLoS Genetics* 17: e1009095.

Paul, J. R., S. N. Sheth, and A. L. Angert. 2011. Quantifying the impact of gene flow on phenotype-environment mismatch: A demonstration with the scarlet monkeyflower *Mimulus cardinalis*. *American Naturalist* 178 (Suppl. 1): s62–s79.

Poorter, H., Ü. Niinemets, L. Poorter, I. J. Wright, and R. Villar. 2009. Causes and consequences of variation in leaf mass per area (LMA): A meta-analysis. *New Phytologist* 182: 565–588.

Ramsey, J., H. D. Bradshaw Jr., and D. W. Schemske. 2003. Components of reproductive isolation between the monkeyflowers *Mimulus lewisii* and *M. cardinalis* (Phrymaceae). *Evolution* 57: 1520–1534.

Rastas, P. 2017. Lep-MAP3: Robust linkage mapping even for low-coverage whole genome sequencing data. *Bioinformatics* 33: 3726–3732.

Reich, P. B., M. B. Walters, and D. S. Ellsworth. 1997. From tropics to tundra: Global convergence in plant functioning. *Proceedings of the National Academy of Sciences, USA* 94: 13730–13734.

Rieseberg, L. H., M. A. Archer, and R. K. Wayne. 1999. Transgressive segregation, adaptation and speciation. *Heredity* 83: 363–372.

Rieseberg, L. H., N. C. Ellstrand, and M. Arnold. 2011. What can molecular and morphological markers tell us about plant hybridization? *Critical Reviews in Plant Sciences* 12: 213–241.

Salguero-Gómez, R. 2017. Applications of the fast-slow continuum and reproductive strategy framework of plant life histories. *New Phytologist* 213: 1618–1624.

Sartori, K., F. Vasseur, C. Violle, E. Baron, M. Gerard, N. Rowe, O. Ayala-Garay, et al. 2019. Leaf economics and slow-fast adaptation across the geographic range of *Arabidopsis thaliana*. *Scientific Reports* 9: 10758.

SAS Institute. 2018. JMP software version 14. SAS Institute, Cary, North Carolina, USA. Website: www.jmp.com.

Sheth, S. N. 2016. Artificial selection reveals high genetic variation in phenology at the trailing edge of a species range. *American Naturalist* 187: 182–193.

Sheth, S. N., and A. L. Angert. 2018. Demographic compensation does not rescue populations at a trailing range edge. *Proceedings of the National Academy of Sciences, USA* 115: 2413–2418.

Shipley, B., M. J. Lechowicz, I. Wright, and P. B. Reich. 2006. Fundamental trade-offs generating the worldwide leaf economics spectrum. *Ecology* 87: 535–541.

Sicard, A., and M. Lenhard. 2011. The selfing syndrome: A model for studying the genetic and evolutionary basis of morphological adaptation in plants. *Annals of Botany* 107: 1433–1443.

Soolanayakanahally, R. Y., R. D. Guy, S. N. Silim, E. C. Drewes, and W. R. Schroeder. 2009. Enhanced assimilation rate and water use efficiency with latitude through increased photosynthetic capacity and internal conductance in balsam poplar (*Populus balsamifera* L.). *Plant, Cell & Environment* 32: 1821–1832.

Stathos, A., and L. Fishman. 2014. Chromosomal rearrangements directly cause underdominant F1 pollen sterility in *Mimulus lewisii–Mimulus cardinalis* hybrids. *Evolution* 68: 3109–3119.

Steyn, W. J., S. J. E. Wand, D. M. Holcroft, and G. Jacobs. 2002. Anthocyanins in vegetative tissues: A proposed unified function in photoprotection. *New Phytologist* 155: 349–361.

Taylor, S. H., D. B. Lowry, M. J. Aspinwall, J. E. Bonnette, P. A. Fay, and T. E. Juenger. 2016. QTL and drought effects on leaf physiology in lowland *Panicum virgatum*. *BioEnergy Research* 9: 1241–1259.

Terashima, I., S.-I. Miyazawa, and Y. T. Hanba. 2001. Why are sun leaves thicker than shade leaves? — consideration based on analyses of CO_2 diffusion in the leaf. *Journal of Plant Research* 114: 93–105.

Thompson, K. A., M. Urquhart-Cronish, K. D. Whitney, L. H. Rieseberg, and D. Schluter. 2021. Patterns, predictors, and consequences of dominance in hybrids. *American Naturalist* 197: E72–E88.

Troth, A., J. R. Puzey, R. S. Kim, J. H. Willis, and J. K. Kelly. 2018. Selective trade-offs maintain alleles underpinning complex trait variation in plants. *Science* 361: 475–478.

Vasseur, F., C. Violle, B. J. Enquist, C. Granier, and D. Vile. 2012. A common genetic basis to the origin of the leaf economics spectrum and metabolic scaling allometry. *Ecology Letters* 15: 1149–1157.

Vile, D., E. Garnier, B. Shipley, G. Laurent, M.-L. Navas, C. Roumet, S. Lavorel, et al. 2005. Specific leaf area and dry matter content estimate thickness in laminar leaves. *Annals of Botany* 96: 1129–1136.

Wright, I. J., P. B. Reich, M. Westoby, D. D. Ackerly, Z. Baruch, F. Bongers, J. Cavender-Bares, et al. 2004. The worldwide leaf economics spectrum. *Nature* 428: 821–827.

Yuan, Y.-W., A. B. Rebocho, J. M. Sagawa, L. E. Stanley, and H. D. Bradshaw Jr. 2016. Competition between anthocyanin and flavonol biosynthesis produces spatial pattern variation of floral pigments between *Mimulus* species. *Proceedings of the National Academy of Sciences, USA* 113: 2448–2453.

Yuan, Y.-W., J. M. Sagawa, V. S. Di Stilio, and H. D. Bradshaw Jr. 2013a. Bulk segregant analysis of an induced floral mutant identifies a MIXTA-like R2R3 MYB controlling nectar guide formation in *Mimulus lewisii*. *Genetics* 194: 523–528.

Yuan, Y.-W., J. M. Sagawa, L. Frost, J. P. Vela, and H. D. Bradshaw, Jr. 2014. Transcriptional control of floral anthocyanin pigmentation in monkeyflowers (*Mimulus*). *New Phytologist* 204: 1013–1027.

Yuan, Y.-W., J. M. Sagawa, R. C. Young, B. J. Christensen, and H. D. Bradshaw Jr. 2013b. Genetic dissection of a major anthocyanin QTL contributing to pollinator-mediated reproductive isolation between sister species of *Mimulus*. *Genetics* 194: 255–263.